International Conference on Renewable Energies and Power Quality (ICREPQ'16)
Madrid (Spain), 4th to 6th May, 2016
Renewable Energy and Power Quality Journal (RE&PQJ)
ISSN 2172-038 X, No.14 May 2016

BIOCARBONS FOR ENERGY CONVERSION AND STORAGE: DEFC$_S$ AND SUPERCAPACITORS APPLICATIONS

A. Cuña[1,2], E. L. da Silva[2], M. R. Ortega[2], C. Radtke[3], N. Tancredi[1], S. C. Amico[4] and C. Malfatti[2]

[1] Cátedra de Fisicoquímica, DETEMA, Facultad de Química, Universidad de la República, Montevideo 11800 (Uruguay)
Phone/Fax number: +598 29248352, e-mail: acuna@fq.edu.uy, nestor@fq.edu.uy

[2] LAPEC/PPGE3M, Universidade Federal do Rio Grande do Sul, Av. Bento Gonçalves, 9500, setor 4, prédio 43427, sala 232 - 91501-970 – Porto Alegre/RS (Brazil)
Phone/Fax number: +55 51 33089406, e-mail: elen.leal@ufrgs.com, ortega.vega@ufrgs.br, celia.malfatti@ufrgs.br

[3] Instituto de Química, Universidade Federal do Rio Grande do Sul, Av. Bento Gonçalves, 9500 - 91501-970 – Porto Alegre/RS (Brazil)
Phone/Fax number: +55 51 33086204, e-mail: claudio.radtke@ufrgs.br

[4] LAPOL/DEMAT, Universidade Federal do Rio Grande do Sul, Av. Bento Gonçalves, 9500, setor 4, prédio 43426, sala 119 - 91501-970 – Porto Alegre/RS (Brazil)
Phone/Fax number: +55 5133089419, e-mail: amico@ufrgs.br

Abstract

Activated biocarbons (aBCs) and activated biocarbon monoliths (aBCMs) were obtained by several procedures in order to study their behaviour as PtSn support for ethanol electro-oxidation, and also for use as an electrode in supercapacitors. The textural and chemical properties of the materials were correlated with the electrochemical behaviour. The prepared *E. grandis* wood based biocarbon materials, have good qualities for use as PtSn catalyst support for DEFCs, and in supercapacitor electrode application. The micropore size and the content of oxygenated functional group have direct incidence on the distribution of the catalyst particles on the aBCs support surface. In consequently, the electrocatalytic behaviour of the PtSn/aBC is affected. The content of oxygenated functional groups also has a marked effect on the supercapacitors electrode behaviour. It was demonstrated that these functional groups are actively involved in the energy storage by the pseudocapacitive phenomenon. The nitric acid treatment is a good method to generate these functional groups on the aBCMs.

Keywords

Energy conversion, Energy storage, Direct Ethanol Fuel Cells, Supercapacitor, Biocarbons

1. Introduction

Direct ethanol fuel cells (DEFCs) are based in ethanol electro-oxidation at low temperature and they constitute an alternative energy conversion system. Besides, supercapacitors are promising electrochemical energy storage devices with important advantages over batteries, including higher power density and larger number of charge/discharge cycles. Carbons and activated carbons are the most widely used materials for supercapacitor electrodes [1] and catalysts support in fuel cells [2] because they can satisfy all the requirements for these applications: high specific surface area, open porosity, high conductivity, electrochemical stability and moderate low cost. Activated carbons are currently prepared from a precursor, such as a polymer, a mineral carbon or some kind of biomass wastes [3]. Regarding the latter, biomass wastes are a renewable source, available in large amounts, and still at low cost [4]. The use of biomass derived carbons (biocarbons) as active electrode materials for supercapacitors and DEFCs has been reported in the last years with promising results [5-7]. The biomass nature and the activation method determine the textural properties, surface chemistry, electrical conductivity and electrochemical performance of the materials. On the other hand, carbon monoliths are pieces of carbon without binders or other additives. They have been tested as supercapacitor electrodes and they show higher electrical conductivity and better structural integrity than the electrodes processed with binders and exhibited excellent electrochemical performance as compared with

conventional electrodes made from powdered activated carbon [8].

Eucalyptus is a tree cultivated over the world that shows the advantage of its rapid growing. Its wood is currently used for manufacturing furniture and for obtaining cellulose paste and allows the preparation of activated carbons with high microporosity [9].

In this work, *Eucalyptus grandis* wood dust was chosen as carbon precursor, and activated biocarbons (aBCs) and activated biocarbon monoliths (aBCMs) were obtained by several procedures including physical activation with CO_2 and chemical activation with $ZnCl_2$. In order to increase the content of oxygenated surface functional groups, which can contribute to increase the electrical capacitance of the material by the pseudocapacitive phenomena, some aBCMs were chemically oxidized with nitric acid. The textural and chemical properties of the carbon materials were determined. Then, aBCs were tested as active PtSn catalysts support for DEFCs and the aBCMs were tested as electrode materials for supercapacitors. The textural and chemical properties of the materials were correlated with the electrochemical behaviour.

2. Materials and methods

A. Carbon material preparation and characterization

aBCs and aBCMs were prepared from *E. grandis* wood. Before the activation, the wood was ground, sifted and then dried at 105 °C for 24 hours. The aBCs were prepared by physical activation with CO_2 (flow 200 cm^3 min^{-1}) at 800 °C for 2 h (p-BC) and chemical activation with $ZnCl_2$ at 900 °C for 1 h (c-BC) in nitrogen atmosphere (200 cm^3 min^{-1}). aBCMs and oxidized activated biocarbon monolith (ox-aBCMs) were prepared from parallelepiped pieces of *Eucalyptus grandis* wood (WMs). The pieces were cut in the transversal direction of the wood tree trunk as described by Cuña et al. [5]. aBCMs were obtained by pyrolysis of wood monoliths (WMs) at 900 ºC for 2 h under N_2 (99.998 %) flow (200 mL min^{-1}) and subsequent activation under CO_2 flow (200 mL min^{-1}) at 800 ºC for 2 h. The heating rate from room temperature to 900 °C was 2 ºC min^{-1}. Ox-aBCMs were obtained by nitric acid oxidation of some aBCMs at 100 °C for 8 h in a 8 mol L^{-1} HNO_3 solution. All the thermal treatments were carried out in a horizontal Carbolite (CTF 12/75) furnace under a controlled gas flow. The used activation methods were based in the previous described procedures [3].

The carbon material texture was determined by N_2 adsorption/desorption isotherm at 77 K, with a Beckman Coulter SA 3100 equipment. For mesoporous samples, Brunauer-Emmet-Teller (BET) model was applied, and the total pore volume (V_T) at relative pressure of 0.99 and specific surface area (S_{BET}) were determined. Average pore diameter (*dp*) was determined by the equation described in [10]. For microporous samples, microporous surface area (S_{mic}), micropore volume (W_o) and the average micropore width (L_0) were determined by the Dubinin-Radushkevich equation [11]. Elemental composition (nitrogen, hydrogen, carbon and sulfur) was determined with a Thermo Scientific Flash 2000 equipment. Ash content was determined according to ASTM D2866/2011 [12]. The oxygen content was determined by difference.

B. Electrocatalysts preparation and characterization

Electrocatalysts synthesis was already explained in a former work [13]. Impregnation/reduction method was employed, using ethylene glycol as reduction agent and $H_2PtCl_6.6H_2O$, $SnCl_2.2H_2O$ salts as catalyst precursors. Adequate amounts of support (aBC) and salts were mixed together to obtain electrocatalysts with a Pt:Sn atomic ratio of 4:1 and a metal charge of 40 wt %. The Rutherford backscattering spectrometry (RBS) analyses were performed using a He^+ beam at 2 MeV produced by TANDEM accelerator of 3 MV. In all the cases, the incidence beam was perpendicular to the sample surface and the detection angle was 165° related to beam direction. In order to determine the catalysts mass percentage in the electrocatalysts, TG was performed on the catalysts supported systems using a Shimadzu TG-50 in dynamic air atmosphere, in the temperature range from 298 to 1123 K using 5 K min^{-1} heating rate, with sample masses between 8.0 and 10.0 mg in platinum crucible. The constant mass at the end of the thermogravimetric curve was related to the amount of catalyst present in the sample. X-Ray diffraction analysis was made with a Philips, X'Pert MPD equipment, operating with Cu-Kα radiation, generated with 40 kV and 40 mA. X-Ray diffractogram allows establishing the crystal structure assumed by the catalyst inside the support. Morphological information for the catalysts was obtained with a FEI Tecnai Spirit Biotwin G2 TEM, operating at 100 kV.

The electrochemically active surface area (EASA) of the electrocatalyst was determined by cyclic voltammetry in 0.5 mol L^{-1} H_2SO_4 solution at 10 mV s^{-1} in the potential range of -0.2 to 0.8 V vs. the saturated calomel electrode (SCE) as described for Carmo et al. [14]. A three electrodes cell with platinum as the counter electrode and Saturated Calomel Electrode (SCE) as the reference electrode, was used in the experiments. As a working electrode, a graphite disk with 0.29 cm^2 in area, which was covered with a mixture of catalyst powder Nafion® was used. The graphite disk was placed in Teflon support to carry out electrochemical analyzes. The preparation procedure for the working electrode consisted in mixing 5 mg of dispersed catalyst particles (supported on carbon) in 2 mL ethanol (Merck) and 25 uL of Nafion (5% by weight, Aldrich). This solution was placed in an ultrasonic bath to homogenize the material and aliquots of the mixture were added to the graphite disk.

Linear sweep voltammetry was done in order to determine the electrochemical behaviour of the catalyst in 1.0 mol L^{-1} ethanol + 0.5 mol L^{-1} H_2SO_4 solution. Measurements were carried out using a three-electrode cell, with platinum wire as counter-electrode and saturated Ag/AgCl as reference electrode. As working electrode a graphite disk was used with a geometric area of 0.29 cm^2, which was coated with a mixture of catalyst powder in Nafion®. The experiments were done with scan rate of 10 mV s^{-1}, in a potential range from -0.2 to 1.0 V. In order to eliminate the oxygen present in the medium, nitrogen was bubbling inside the solution since 10 minutes before. All the electrochemical measurements were performed at

25 °C, on a potentiostat/galvanostat AUTOLAB PGSTAT 302N.

C. *Supercapacitor electrodes preparation and characterization*

Two-electrode Swagelok®-type cells having two tantalum rods as current collectors were used for galvanostatic charge/discharge measurements. A glassy microfiber paper (Whatman 934 AH) was chosen as separator. aBCM and ox-aBCM with a cross-section area of 0.40 – 0.48 cm^2 and length of 0.20 cm were chosen as electrodes. The weight of the electrodes was between 41 mg and 47 mg. 2 mol L^{-1} H_2SO_4 solution was used as electrolyte. Before the cell assembly, the electrodes were soaked in the electrolyte under vacuum (≈ $3 \cdot 10^3$ Pa) for 24 h.

The specific and volumetric capacitances were determined from galvanostatic charge/discharge measurements in the voltage range of 0 V - 1 V at current densities in the range 1-70 mA cm^{-2}. The specific capacitance C_s was determined at each current according to the equation: $C_s = 2 \cdot I \cdot t_d / E_2 \cdot m_e$, where I is the current applied, t_d is the discharge time, E_2 is the voltage range during the discharge, and m_e is the mass of one carbon monolith. The volumetric capacitance C_V was determined according to the equation: $C_V = C_s \cdot \rho$, where ρ is the bulk density. The bulk density was determined by using an analytical balance and by measuring the geometrical dimensions of the electrodes. Equivalent series resistance (ESR) was determined according to $ESR = I/2 \cdot E_1$ were E_1 is the initial voltage drop in the discharge.

For cyclic voltammetries, the carbon monolith was composed into a three-electrode system as the working electrode. The reference and the counter electrodes were Ag/AgCl and a Pt wire, respectively. The voltammograms were obtained at room temperature in the range of -0.2 to 0.8 V at different scan rates (0.1, 0.5, 1, 2 y 5 mV s^{-1}). The current density in A g^{-1} was calculated from the current applied and the mass of the carbon monolith.

All electrochemical measurements were carried out at the same temperature and with the same equipment described in the previous section.

3. Results and discussion

A. *Textural and elemental analysis*

The results of the textural and elemental analysis of the aBCs and aBCMs are shown in the Table I. With the exception of the p-BC, all the samples have a microporous microstructure while the p-BC had a texture located at the bottom limit of mesoporosity with a 2.4 nm pore diameter. aBCMs have a smaller pore size and specific surface area than the aBCs, probably due to increased contraction of the monolithic structure of wood in the case of monoliths with respect to wood powder. For the monoliths, pore size slightly decrease after the nitric acid-based treatment. This could be explained by the fixation of surface oxygen on the walls which lead to a decrease in average pore diameter [15]. The bulk density of the aBCMs is very similar, 0.50 and 0.43 g cm^{-3} for aBCM and ox-aBCM respectively. The biocarbon materials have an oxygen content of around 10 %. This oxygen corresponds to the surface oxygen functional groups present in the carbons. The higher carbon content and the lower oxygen and hydrogen content of the c-BC with respect to the p-BC is expected due to the higher c-BC maximum activation temperature (900 °C) compared to the p-BC (800 °C), which determines a higher oxygenated and hydrogenated compounds devolatilization of the precursor material [6].

The nitric acid treatment of the aBCMs produces a significant increase in the oxygen content (from 13.9 to 23.2 %), and to a lesser extent, an increase in the nitrogen content (0.2 to 0.5 %). It indicates the effectiveness of the nitric acid treatment in modifying the carbon monoliths surface in agreement with previous research [15].

B. *PtSn* nanocatalysts *supported on activated biocarbons (aBCs): morphology, structure and electrocatalytic performance*

It is found that the composition determined by RBS analysis was fairly similar to the nominal composition shifts within the experimental error. The amount of catalysts supported on the different activated carbons are according to the metallic charge (40 wt %) used in the synthesis. These results suggest that the impregnation/ reduction method using ethylene glycol as a reducing agent is a suitable method for obtaining particles of PtSn.

Table I. Textural and elemental analysis of biocarbon materials

	Textural Analysis				**Elemental Analysis (mass percentage, dry basis)**					
Sample	**V_T or W_o (cm^3/g)**	**S_{BET} (m^2/g)**	**S_{mic} (m^2/g)**	**d_p or L_o (nm)**	**C**	**H**	**N**	**S**	**Ash**	**O***
p-BC	0.47	787	-	2.4	82.2	1.7	0.0	0.0	6.1	10.0
c-BC	0.51	-	752	1.3	89.8	0.9	0.0	0.0	0.6	8.7
aBCM	0.25	-	603	0.8	83.2	1.2	0.2	0.0	1.5	13.9
Ox-aBCM	0.26	-	643	0.7	73.3	1.6	0.5	0.0	1.4	23.2

*by difference

In Figure 1 it can be seen the diffraction peaks located at 39°, 46°, 68°, 81° and 87° which correspond to the planes (1 1 1) (2 0 0) (2 2 0) (3 1 1) and (2 2 2) of platinum, representing a typical platinum cubic face centered crystal structure [14, 16, 17]. Lattice parameter and crystallite size computations are explained in former work [7]. The electrocatalysts studied in this work has greater average lattice parameter value "a" (3.3 and 3.5 Å

for the c-BC and p-BC respectively) and thus dilatation of the crystallite lattice as compared with pure platinum values [13]. This result is in agreement with the literature were the PtSn peak displacement was assigned to the alloying between platinum and tin, indicating a PtSn alloy formation and not only a Pt or Sn separately deposition [18, 19].These results show that the ethylene glycol reduction method produces nanoparticles in the desired size range for applications in fuel cells [14].

PtSn support surface distribution and particle size were estimated from examination of TEM images shown in Figure 2. The particles have average sizes of 2.5 nm for p-BC and 3.5 nm for c-BC. These results agree with those reported for PtSn alloy supported on different types of carbon materials [20, 21] and is also consistent with the mean crystallites sizes calculated from XRD data.

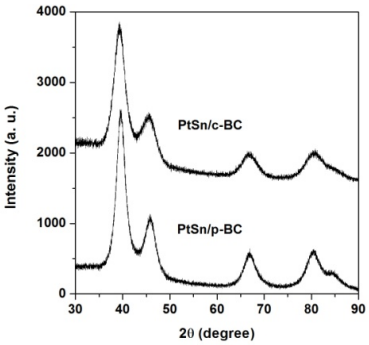

Figure 1. X-ray diffraction patterns of PtSn/BC electrocatalysts.

In TEM images, it can also be seen that the PtSn particles are dispersed throughout the whole support. aBCs have microporous surface area with narrow pores, therefore, a great part of its surface area will not be accessible for the reactant during the synthesis of the electrocatalyst, especially for large molecules as $PtCl_6^{2-}$ (anion precursor in the PtSn) [22]. This may determine a lower surface area available for creating nucleation sites, which allow localization throughout the whole aBC support. In addition, the highest content of oxygenated functional groups of the aBCs, determined by elemental analysis (Table I), may have a negative effect on the degree of catalyst distribution on the support surface [23]. Román-Martínez et. al [24] reported the reduction of Pt from the $PtCl_6^{2-}$ precursor on the carbon basal planes. In this sense, there is an hindrance stablished by the oxygenated surface functional group, for the metallic precursor to reach those carbon basal planes, due to the repulsion between the catalyst precursor molecules and the oxygen atoms on the biocarbon surface. This behavior it could also apply for the PtSn catalyst, since Pt is the main component of the alloy.

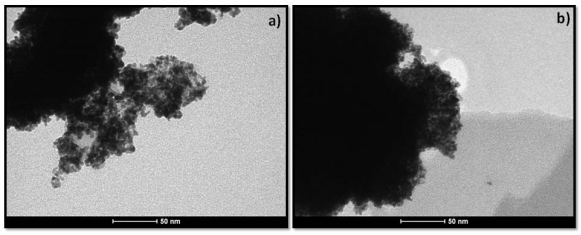

Figure 2. Images obtained from TEM a) PtSn/p-BC and b) PtSn/c-BC.

The voltammetries obtained in the absence of ethanol (not shown), display the typical profile of the hydrogen absorption/desorption on Pt. All catalysts showed a peak between -0.2 V and 0.1 V vs SCE electrode which is in agreement with previous reports [14]. The corresponding values of EASA, expressed per unit mass of Pt, are 65.07 and 52.24 m^2 gPt^{-1}. The catalysts supported on the physical p-BC have slightly higher EASA than those supported on the c-BC. Figure 3 shows the results of the linear sweep voltamogrammetries at 10 mV s^{-1} obtained for ethanol electro-oxidation on PtSn/aBCs electrocatalysts at 1 mol L^{-1} of ethanol concentration. Both samples have similar behavior in terms of onset potential (E_{onset} = 0.2 V) and the maximum current density. The current density for potentials above 0.8 V is slightly higher for the p-BC than the c-BC in accordance with their slightly higher EASA.

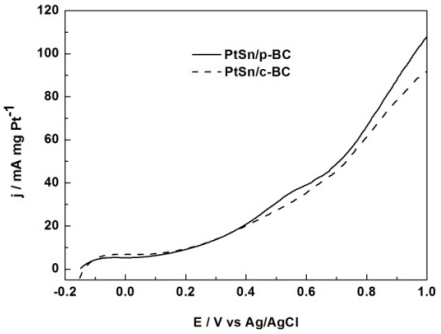

Figure 3. Linear sweep voltammograms of different electrocatalysts.

C. Activated biocarbon monoliths ($aBCM_s$) as supercapacitor electrodes

The dependence of the specific (gravimetric) and volumetric capacitance as a function of the current density is shown in Fig. 4a and 4b, respectively. At low current density (1 mA cm^{-2}), the oxidized monolith (ox-aBCM) has higher value than the non-oxidized monolith (aBCM), 187 F g^{-1} or 80 F cm^{-3} and 89 F g^{-1} or 49 F cm^{-3} respectively. This difference cannot be assigned to differences in the textural properties of materials, since both types of materials have the same pore size and similar surface areas (Table I). If we consider the value of the electrochemical double-layer for similar materials (0.10 F m^{-2} in acidic electrolyte) [1,24] and the S_{mic} values, the expected value for the electric double-layer capacitance is 60 and 64 F g^{-1} for the aBCM and ox-aBCM respectively. It corresponds to 67 and 31 % of the total capacitance. The difference between these values and those obtained for the total capacitance at 1 mA cm^{-2} (187 F g^{-1} and 89 F g^{-1}), must correspond to the pseudocapacitive contribution. This pseudocapacitive contribution is more important for the oxidized monolith (69% of the total capacitance) than the non-oxidized one (33%). The presence of reversible redox reactions is clearly evidenced in the cyclic voltammetry obtained for ox-aBCM (Figure 5). The voltammogram of this monolith shows peaks between 0.3 V and 0.6 V vs. Ag/AgCl electrode. These peaks can be assigned to

reversible reactions of the surface functional groups, in particular quinone and hydroxyl groups [1, 25]. This is consistent with the elemental analysis results, which demonstrates an increase of oxygen content after the oxidative treatment. It has also been reported that carboxyl, hydroxyl and nitro functional groups, can improve the wettability of carbon facilitating the electrolyte accessibility in the carbon pores [15, 26]. This will influence the double-layer capacitance that can be obtained, especially in fine-pore high-area materials [26].
The presence of oxygenated groups at the carbon surface and their negative contribution to the electrical conductivity was already reported [6]. The higher ESR value obtained for the ox-aBCM sample (6.8 Ω) than for aBCM (1.1 Ω), suggests that the introduction of oxygenated functional groups through oxidation makes the material more electrically resistive.

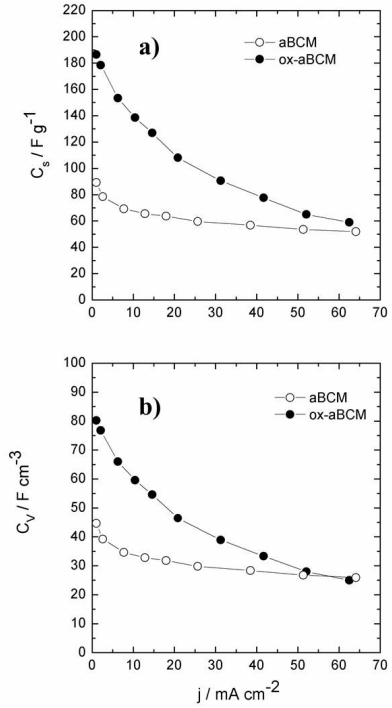

Figure 4. Specific capacitance (a) and volumetric capacitance (b) vs current density for activated biocarbon monolith (aBCM) and oxidized activated biocarbon monolith (ox-aBCM).

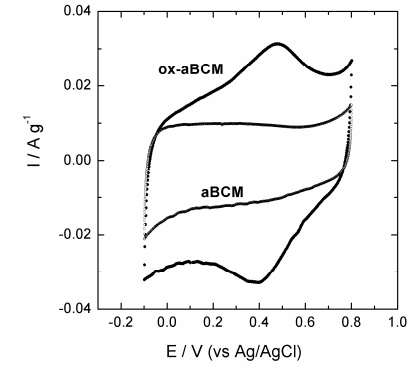

Figure 5. Cyclic voltammetry at the scan rate of 0.1 mV s^{-1} recorded on the activated carbon monolith (aBCM) and oxidized activated carbon monolith (ox-aBCM).

The Ragone plot is shown in Figures 6a and 6b. The gravimetric and volumetric energy densities W_S and W_V are calculated according to: $Ws = ½ C_S \cdot E_2^2$ and $W_V = ½ C_V \cdot E_2^2$, where C_S and C_V are the specific and volumetric capacitances measured at each current density and E_2 is the voltage range during the galvanostatic discharge at each current density. The gravimetric and volumetric power densities P_S and P_V are calculated as: $P_S = W_S/t_d$ and $P_V = W_V/t_d$, where t_d is the discharge time. Comparing the carbon monoliths, it is observed that the oxidized monolith (closed symbol) show higher energy, up to 25 Wh kg^{-1} and 11 Wh L^{-1}, than the non-oxidized one (open symbol), up to 12 Wh kg^{-1} and 6 Wh L^{-1}. These values are better than those reported by other authors for similar carbon monoliths [27]. The highest power density of P_S = 756 W kg^{-1} and P_V = 378 W L^{-1} is achieved for the non-oxidized monolith. The higher power density is in agreement with the larger contribution of the double layer to the overall specific capacitance and the less electric resistance of the oxidized sample as compared to the non-oxidized.

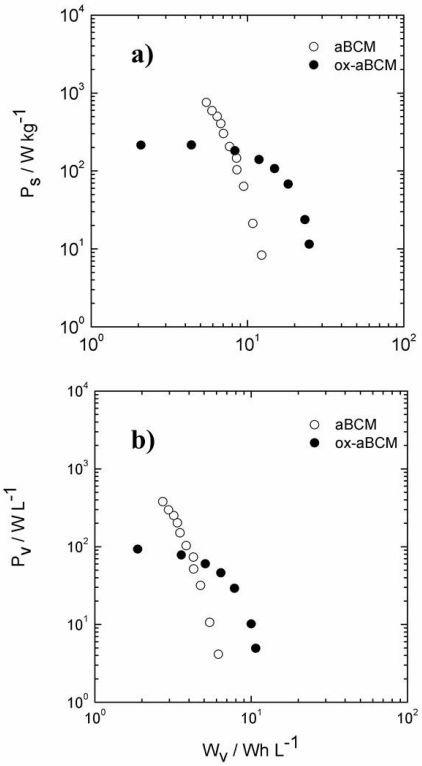

Figure 6. (a) Gravimetric power density vs. gravimetric energy density. (b) Volumetric power density vs. volumetric energy density.

4. Conclusions

The prepared *E. grandis* wood based biocarbon materials, have good qualities for use as PtSn catalyst support for DEFCs, and in supercapacitor electrode application.
The aBCs and aBCMs showed high specific surface area associated to microporosity. The micropore size and the content of oxygenated functional group have direct incidence in the distribution of the catalyst particles on

the aBCs support surface. In consequently, the electrocatalytic behavior of the PtSn/aBC is affected. The content of oxygenated functional groups also has a marked effect on the supercapacitors electrode behavior. It was demonstrated that these functional groups are actively involved in the energy storage by the pseudocapacitive phenomenon. In this regard, it has been demonstrated that the oxidative treatment with nitric acid is a good method to generate these functional groups on the aBCMs.

Acknowledgements

Authors would like to thank the financial support of the Brazilian CAPES/UdelaR Program (EDITAL Nº 40/2011) and the CNPq. A. Cuña thanks the Brazilian CAPES for the grant received (Bolsista CAPES/Brasil).

References

[1] F. Béguin, E. Frąckowiak. Supercapacitors: Materials, Systems and Applications. Wiley-VCH Verlag GmbH & Co, Weinheim (2013).

[2] P. Serp, J. L. Figueiredo, Carbon Materials for Catalysis, Wiley, New Jersey (2009).

[3] H. Marsh H., R. Rodríguez-Reinoso F. Activated carbons. Elsevier, Oxford, UK (2006).

[4] P. Kalyani and A. Anitha, "Biomass carbon & its prospects in electrochemical energy systems". Int J Hydrogen Energy 2013, Vol. 38, pp. 4034-4045.

[5] A. Cuña, N. Tancredi, J. Bussi, V. Barranco, TA. Centeno, A. Quevedo, JM. Rojo, "Influence of wood anisotropy on the Electrical and Electrochemical Performance of Biocarbon Monoliths as Supercapacitor Electrode". Journal of the Electrochemical Society 2014, Vol. 161, pp. A1806-A1811.

[6] A. Cuña, N. Tancredi, J. Bussi, C. Deiana, MF. Sardella, V. Barranco and JM. Rojo, "*E. grandis* as a biocarbons precursor for supercapacitor electrode application". Waste and Biomass Valorization 2014, Vol. 5, pp. 305-313.

[7] EL. da Silva, MR. Ortega Vega, PS. Correa, A. Cuña, N. Tancredi and CF. Malfatti, "Influence of activated carbon porous texture on catalyst activity for ethanol electro-oxidation". International Journal of Hydrogen Energy 2014, Vol. 39 pp. 14760-14767.

[8] A. Garcia-Gomez, P. Miles, TA. Centeno, JM. Rojo, "Why Carbon Monoliths are Better Supercapacitor Electrodes than Compacted Pellets". Electrochem Solid-State Lett 2010, Vol. 13, pp. A112-A114.

[9] A. Amaya, N. Medero, N. Tancredi, H. Silva, C. Deiana, "Activated carbon briquettes from biomass materials". Bioresource Technology 2007, Vol. 98, pp. 1635-1641.

[10] S. Lowell, J. E. Shields. Powder Surface Area and Porosity, Chapman and Hall Ltd, London (1984).

[11] F. Stoeckli, TA. Centeno, "Optimization of the characterization of porous carbons for supercapacitors". J. Mater. Chem. A 2013, Vol. 1, pp. 6865-6873.

[12] D28 Committee. Test Method for Total Ash Content of Activated Carbon. ASTM International; 2011.

[13] PS. Correa, EL. Silva, RF. Da Silva, C. Radtke, B. Moreno, E. Chinarro, CF. Malfatti, "Effect of decreasing platinum amount in Pt–Sn–Ni alloys supported on carbon as electrocatalysts for ethanol electrooxidation". Int J Hydrog Energy 2012, Vol. 37, pp. 9314–9323.

[14] M. Carmo, AR. dos Santos, JGR. Poco, M. Linardi, "Physical and electrochemical evaluation of commercial carbon black as electrocatalysts supports for DMFC applications". J Power Sources 2007, Vol. 173, pp. 860–866.

[15] MC. Liu, LB. Kong, P. Zhang, YC. Luo, K. Long, "Porous wood carbon monolith for high- performance supercapacitors". Electrochim Acta 2012, Vol. 60, pp. 443-448.

[16] W. Zhou, Z. Zhou, S. Song, W. Li, G. Sun, P. Tsiakaras, et al. "Pt based anode catalysts for direct ethanol fuel cells". Appl Catal B Environ 2003, Vol. 46, pp. 273–285.

[17] M. Chatterjee, A. Chatterjee, S. Ghosh, I. Basumallick, "Electro-oxidation of ethanol and ethylene glycol on carbon-supported nano-Pt and -PtRu catalyst in acid solution". Electrochimica Acta 2009, Vol. 54, pp. 7299–7304.

[18] F. Colmati, E. Antolini, ER. Gonzalez, "Ethanol oxidation on a carbon-supported Pt75Sn25 electrocatalyst prepared by reduction with formic acid: Effect of thermal treatment". Appl Catal B Environ 2007, Vol. 73, pp.106–115.

[19] JH. Kim, SM. Choi, SH. Nam, MH. Seo, SH. Choi, WB. Kim, "Influence of Sn content on PtSn/C catalysts for electrooxidation of C1–C3 alcohols: Synthesis, characterization, and electrocatalytic activity". Appl Catal B Environ 2008, Vol. 82, pp. 89–102.

[20] JCM. Silva, LS. Parreira, RFB. De Souza, ML. Calegaro, EV. Spinacé, A. Oliveira Neto, MC. Santos, "PtSn/C alloyed and non-alloyed materials: Differences in the ethanol electro oxidation reaction pathways". Applied Catalysis B: Environmental 2011, Vol. 110, pp. 141–147.

[21] JM. Léger, S. Rousseau, C. Coutanceau, F. Hahn, C. Lamy, "How bimetallic electrocatalysts does work for reactions involved in fuel cells? Example of ethanol oxidation and comparison to methanol". Electrochimica Acta 2005, Vol. 50, pp. 5118–5125.

[22] P. Serp, B. Machado, Nanostructured Carbon Materials for Catalysis. Royal Social of Chemistry, Londres (2015).

[23] L. Calvillo, V. Celorrio, R. Moliner, AB. Garcia, I. Camean, MJ. Lazaro. "Comparative study of Pt catalysts supported on different high conductive carbon materials for methanol and ethanol oxidation". Electrochimica Acta 2013, Vol. 102, pp. 19–27.

[24] MC. Roman-Martinez, D. Cazorla-Amoros, A. Linares-Solano, C. De Lecea, S-M. Yamashita, "H and Anpo M. Metal Support Interaction in Pt/C Catalysts. Influence of the support surface chemistry". Carbon 1995, Vol. 33, pp.3–13.

[25] A. Sliwak, B. Grzyb, J. Cwikła, G. Gryglewicz, "Influence of wet oxidation of herringbone carbon nanofibers on the pseudocapacitance effect". Carbon 2013, Vol. 64, pp. 324-333.

[26] BE. Conway. Electrochemical supercapacitors. Scientific Fundamentals and Technological applications. Kluwer Academic/Plenum Publishers; New York (1999).

[27] V. Ruiz, C. Blanco, R. Santamaría, JM. Ramos-Fernández, M. Martínez-Escandell, A. Sepúlveda-Escribano, F. Rodríguez-Reinoso, "An activated carbon monolith as an electrode material for supercapacitors". Carbon 2009, Vol. 47, pp. 195-200.